Anisotropic characteristics analysis of 3D-printed optics

Tobias Grabe* **, Tobias Biermann* ***, Maximilian Bayerl*, Roland Lachmayer* ** ***

*Institute of Product Development, Leibniz University Hannover, D-30823 Garbsen
**GROTESK, D-30167 Hannover
***Cluster of Excellence PhoenixD, D-30167 Hannover

mailto:grabe@ipeg.uni-hannover.de

The Additive Manufacturing of transparent materials enables cost efficient rapid prototyping of optically transparent components. The components are built layer-by-layer which can cause anisotropic optical properties. We present the quantitative analysis of anisotropic imaging and its dependence on the layer thickness of MJM-printed transparent samples.

1 Introduction

For the design of optical transparent elements, Additive Manufacturing offers a great potential to produce cost efficient individually adapted freeform optics [1][2]. One of the most common and commercially available printing processes for transparent polymers is Multi-Jet Modeling (MJM) [3]. During the layer-by-layer curing of the material, its optical properties are changed. Thus, the optically scattering effects in the materials volume can be identified [4]. Without quantification of these properties, the design quality of Additive Manufactured optics in products is limited [5]. In this work, the impact of the layer thickness on the optical volume scattering of MJM-manufactured parts will be quantitatively evaluated.

2 Multi-Jet Modeling

1) Jetting head
2) UV light
3) Build material
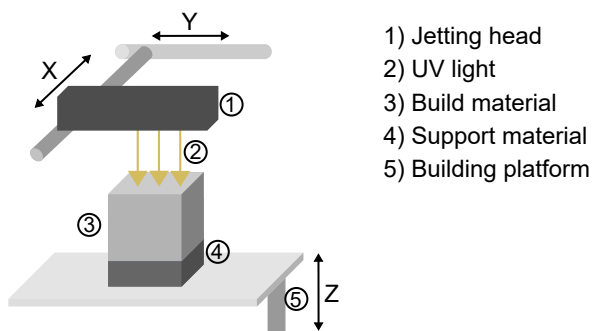4) Support material
5) Building platform

Fig. 1 Multi-Jet Modeling setup

The samples were manufactured on an Objet30 Pro. In MJM the print heads are applying a photopolymer drop-by-drop on a platform, which are cured by UV light (Fig. 1). For printing, the resin VeroClear is used. In the horizontal plane the printing resolution is 600 dpi.

3 Experimental Set-up

Equilateral cubes with an edge length of 25 mm are printed with 16 µm and 32 µm layer thickness and all planes are polished. For the analysis a laser beam is propagating through a cube perpendicular to the plane in X-, Y- and Z-axis orientation. The orientations are defined in Fig. 1. The beam is projected on a surface at 143 mm distance to the cube and is detected by a CMOS sensor. For the measurement a Helium-Neon laser with a wavelength of λ = 632 nm at a maximum power of 1 mW, a Gaussian power distribution and a collimation beam diameter of 2 mm is used.

4 Results

The projected beam profile which results of the laser beam propagating through the sample from different directions is shown in Fig. 2 for a layer thickness of 16 µm. Here, the anisotropic optical properties of the transparent polymer samples are visible. For quantitative analysis, the coordinate central point is defined at the maximum intensity of the scattered light.
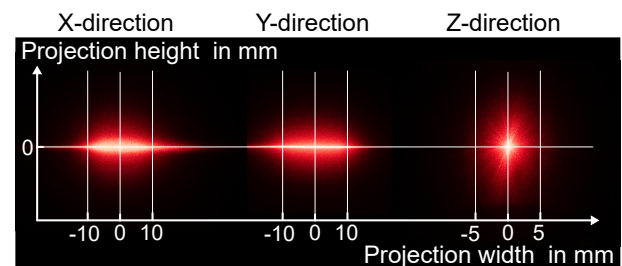

Fig. 2 Scattering patterns on the projection surface.

The intensity matrix **I** shown in Eq. 1 is derived from the sensor data where $i_{h,w}$ denotes the brightness value of a pixel on the sensor. Here, h denotes the vertical position and w the horizontal position of the pixels on the sensor array. The evaluation for the vertical axis is explained exemplary. The normalized energy $f_I(h)$ along the horizontal axis is calculated by the sum of the vertical matrix entries according to Eq. 2.

$$\mathbf{I} = i_{h,w} = \begin{pmatrix} i_{1,1} & \cdots & i_{1,m} \\ \cdots & \cdots & \cdots \\ i_{n,1} & \cdots & i_{n,m} \end{pmatrix} \qquad (1)$$

$$f_I(h) = \sum_{w=1}^{m} i_{h,w} \qquad (2)$$

The measurement results for the vertical (h) and horizontal (w) matrix analysis for laser beam crossing a cube with 16 μm and 32 μm layer thickness in X-, Y- and Z-direction are shown in Fig. 3 and Fig. 4. Here, the results for $f_I(w)$ are normalized to the global maximum value of all measurements.
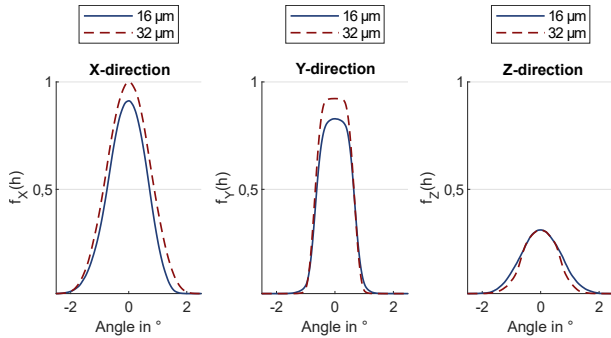

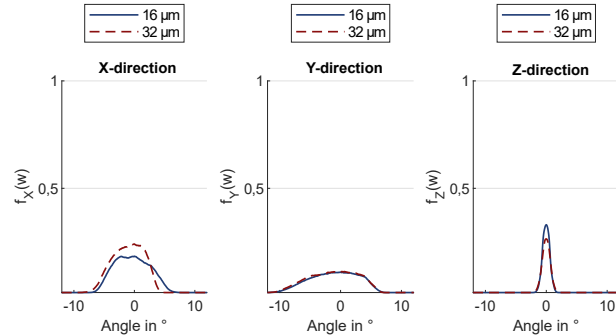**Fig. 3** *Normalized intensity profile (projection height)*

Fig. 4 *Normalized intensity profile (projection width)*

When the laser beam is crossing the sample in X-direction for $f_x(h = 0)$ a value of 1 and $f_x(w = 0)$ = 0.23 is detected for a layer thickness of 32 μm. For a layer thickness of 16 μm a value of $f_x(h = 0)$ = 0.91 and $f_x(w = 0)$ = 0.17 is determined. A scattering cone angle of approximately 2° for vertical scattering and 5° for horizontal scattering can be detected. In Y-direction, a maximum of $f_y(h = 0)$ = 0.92 and $f_y(w = 0)$ = 0.10 for a layer thickness of 32 μm and maximum of $f_y(h = 0)$ = 0.83 and also $f_y(w = 0)$ = 0.10 is determined for a layer thickness of 16 μm. Here, a smaller scattering cone angle of approximately 1° for vertical scattering and 8° for a non-symmetric horizontal scattering can be detected. In Z-direction a maximum of $f_z(h = 0)$ = 0.30 for the two analyzed layer thicknesses is detected. Further, $f_z(w = 0)$ = 0.32

for 16 μm and $f_z(w = 0)$ = 0.25 for 32 μm layer thickness is determined. The doubled layer thickness leads to a decreasing of the vertical scattering cone angle from 2° to 1.5° while the horizontal cone angle remains stable with 1.5°.

5 Discussion and Outlook

In this paper, an initial analysis of the impact of the layer thickness on the optical volume scattering of MJM-manufactured parts is performed. The optical scattering of transparent MJM-printed parts depends on the sample's orientation during the manufacturing process. When the laser beam is crossing the sample in X- and Y-direction, a line-shaped scattering pattern occurs. The normalized energy which is transmitted through the sample along these directions is significantly increased when a larger layer thickness is used for sample manufacturing. However, in Z-direction an increased layer thickness shows a minor decrease of the normalized energy.

By transferring these results into a simulation, MJM-printed optical components can be used to selectively utilize these properties for the use in optical products. Thus, potentially the use of MJM-printed parts for novel, tailored designed optical components can be improved majorly.

6 Acknowledgment

References

[1] T. Grabe, Y. Li, H. Krauss, A. G. Wolf, J. Wu, C. Yao, Q. Wang, R. Lachmayer, and W. Ren, "Freeform optics design for Raman spectroscopy," in *Photonic Instrumentation Engineering VII*, Y. Soskind and L. E. Busse, eds. (SPIE, 2020).

[2] R. Lachmayer, R. B. Lippert, and S. Kaierle, *Konstruktion für die Additive Fertigung 2018* (Springer Berlin Heidelberg, Berlin, Heidelberg, 2020).

[3] G. Leuteritz, R. B. Lippert, K. Rettschlag, and R. Lachmayer, "Comparison of Additive Manufacturing techniques regarding mechanical and optical properties," (DGaO, 2018).

[4] M. Rank, A. Horsak, M. Kudlek, J. Nuding, S. Pekrul, and A. Heinrich, "Diffraktive Effekte an additiv gefertigten optischen Elementen," (DGaO, 2017).

[5] M. Rank and A. Heinrich, *3D Printing of Optics*, vol. SL39 (SPIE, 2018).